Cumhuriyet University Faculty of Science
Science Journal (CSJ), Vol.34, No.3 (2013)

ISSN: 1300-1949

Experimental determination of structural and electrical properties for constant tin concentrations in the Pb-Al-Sn composite system

C. ALPER BİLLUR[a,*], B. SAATÇI[a], M. ARI[a], and A. T. ALTINCI[a]

[a]*Department of Physics, Erciyes University, Kayseri, 38039 Turkey*

Received: 14.11.2013; Accepted: 02.12.2013

Abstract. For the first time, the structural and electrical properties of Pb-Al-Sn composite system for constant tin concentrations were investigated in this work. The electrical conductivity of the samples depending on temperature was measured by four-point probe, and it was found that the conductivity decreases almost linearly with the temperature. The structural properties of the samples were determined by Scanning Electron Microscope (SEM), X-ray diffraction (XRD) and Energy Dispersive X-ray Analysis (EDX). The SEM micrographs of the samples illustrated smooth surfaces with a clear grain boundary. The crystal structure of the samples was indexed in face-centered cubic (fcc) by using XRD data. The cell parameters and the grain sizes were determined from the XRD patterns. In addition, the temperature coefficients of electrical resistivities were obtained determined, which were independent of the compositions of the composite system.

Keywords: Electrical conductivity, crystal structure, X-ray diffraction, electron microscopy.

1. INTRODUCTION

We found a significant amount of research in the literature dedicated to the application areas of Al-Sn, Pb-Sn and Al-Pb binary metallic alloys but clear and authentic information about the uses of Pb-Al-Sn composite system is not yet available. Al-Pb and Al-Sn are Al-based alloys, known for their wide use in sliding bearing applications, good load carrying capacity, fatigue resistance, and wear resistance sliding properties. As compared to other bearing alloys, Al-Pb alloys are used because they possess superior qualities, such as superior friction properties, low cost of production, high thermal conductivity and high corrosion resistance [1-3]. Lead is soft and much cheaper and more freely available than tin. The common use of Pb-Sn alloys can be seen in the production of positive and negative grids, connectors, and in post and strap components in both VRLA (valve regulated lead acid) and SLI (starting, lighting and ignition) batteries which have wide applications in automotive and telecommunication industries [4-6].

* Corresponding author. *Email address*: cananbillur@erciyes.edu.tr (C. Alper Billur)
Tel.: +90 352 207 66 66 /33 129; Fax: +90 352 207 66 66

So far, the crystal lattice parameters and crystal structure have been determined using X-ray scattering studies with different methods [7-15] for various systems. In addition, the grain sizes of the samples were obtained by evaluating the peaks [9, 16]. For the first time, the temperature dependences of electrical properties, grain size, the crystal structure and lattice parameters of Pb-Al-Sn composite system (Pb-39 wt. % Al-20 wt. % Sn, Pb-38 wt. % Al-20 wt. % Sn, Pb-37 wt. % Al-20 wt. % Sn, and for Pb-36 wt. % Al-20 wt. % Sn) were examined in this study. The XRD, SEM and EDX methods were utilized to determine the microstructure properties. SEM micrographs were used in order to analyze the microstructure of the alloys. Finally, the temperature coefficients of resistivity were determined.

2. EXPERIMENTAL SECTION

2.1. Sample Preparation

The details of the apparatus which was used to prepare the Pb-Al-Sn composite system samples are given in the refs [17-19]. A specially designed graphite crucible was used to obtain the samples, The Pb-Al-Sn composite samples (for constant tin concentrations: Pb-39 wt. % Al-20 wt. % Sn, Pb-38 wt. % Al-20 wt. % Sn, Pb-37 wt. % Al-20 wt. % Sn, and Pb-36 wt. % Al-20 wt. % Sn) were prepared from 99.99 % pure Al, Pb and Sn. First of all, sufficient amounts of the pure materials were chemically cleaned, dried, weighed and then dissolved in a vacuum furnace. Later, after many stirrings, the molten metal was poured into a graphite crucible (30 mm diameter) held in a specially constructed casting furnace. Finally, solidification of the composite system was carried out directionally from bottom to top so that the crucible was completely filled and could be taken out afterwards.

2.2. Structural Property Measurements

The SEM and EDX measurements were conducted after the samples obtained were ground and polished using standard techniques. The characterization of the microstructures of the samples was performed by an LED 440 SEM equipped with an EDX spectrometer along with a computer-controlled image analyzer. A backscatter detector was used to take SEM micrographs from the best contrast between the existing phases. After going through each electrical measurement, the EDX spectrometer was used to determine the chemical compositions of the samples under investigation with a possible error of up to 1%.

The crystal structure and lattice parameters were determined by using a computer-interfaced Bruker AXS D8 advanced diffractometer, operated in a Bragg-Brentano geometry (CuK_α λ: 1.54059 A, graphite monochromator, 40 kV and 40 mA) over an angular range of $10^o \leq 2\theta \leq 90^o$. This was used to record the XRD data of the samples of Pb-Al-Sn composite systems. The diffractometer had a divergence

and a receiving slit of 1mm and 0.1mm, respectively. The diffraction patterns were scanned in 0.002^{o} (2θ) steps and the diffracted beams were counted with a NaI (Tl) scintillation detector. The XRD patterns measured were thus quickly and easily compared with the reference data by using the DiffracPlus EVA and WinIndex softwares. The indexing of the XRD patterns of the samples was carried out by DICVOL91 computer program.

The grain size of the samples was also calculated from the higher intensity peaks of the XRD pattern (111), (200), (222), (331) using the Scherrer formula with the help of the DiffracPlus EVA and TOPAS 2 computer programs. The values of the grain sizes were determined by using the Scherrer equation

$$t = \frac{B\lambda}{\beta \cos\theta} \tag{1}$$

Where t is the grain size, B is a constant which is taken as 0.9, λ is the X-ray wavelength used, β is the angular line width at half-maximum intensity in radians and θ is the Bragg angle [20].

2.3. Electrical Measurements

The four-point probe method was used in order to measure the electrical conductivity of the samples. The use of the four-point probe measurement technique eliminated the measurement errors due to probe resistance, the spreading resistance under each probe, and the contact resistances between each metal probe and material [21].

For online data acquisition and processing, the measuring unit was interfaced with a PC. A constant current was provided by a Keithley 2400 sourcemeter and a Keithley 2700 multimeter with a 7700 mutiplexer data logger card was used to detect the potential drop, current and temperature of the sample. Pt wires with a 0.5mm diameter were used as current and potential probes. The standard conversion method [17-19] was used for the calculation of electrical conductivity from the detected current and voltage drop. A controllable Nabertherm furnace was used to adjust the temperature of the sample. The temperature of the samples was also measured using a 0.5 mm standard K type thermocouple which was placed very close to the sample. To carry out the electrical measurements, the sample was cut transversely into ~ 3-5 mm long sections and these specimens were ground with 180-2400 grid SiC paper before mounting. Temperature range from room temperature to just above melting point was observed in the measurements of the circular-shaped samples with a typical 12.5 mm diameter.

In addition, the temperature coefficient of resistivity (TCR) of the Pb-Al-Sn composite systems was also estimated by using the electrical resistivity results between 30^o – 180^o C by using the following equation:

$$\alpha_\rho = (\frac{1}{\rho_1})(\frac{d\rho}{dT}) = (\frac{1}{\rho_1})(\frac{\Delta\rho}{\Delta T}) \quad (2)$$

where α_ρ is the TCR in the temperature between $\Delta T=T_2-T_1$ and $\Delta\rho=\rho_2-\rho_1$, ρ_1 is the resistivity at T_1 and ρ_2 is the resistivity at T_2.

3. RESULTS AND DISCUSSION

SEM micrographs were used to obtain the microstructures of the samples. As shown in Figure 1a, the pure Pb and the Pb-Al-Sn composite system have a polycrystalline structure and no impurities, porosities, cracks, holes or structural defects are not found on the SEM images. Significant and similar characteristics in terms of the surfaces, morphologies and grain structure of the samples were found. As shown in Figure 1b, the results of the EDX analysis illustrate a typical EDX pattern and account for the relative analysis of the samples. In the results of the EDX analysis the Al, Pb an Sn peaks were clearly seen and the composition had similarities with those taken after the electrical measurements. The quantitative chemical composition EDX analysis of various selected regions in the solid phase of the Pb-38 wt. % Al-20 wt. % Sn sample was also done and is given in Figure 2. The Al-rich, Sn-rich and Pb-rich phases were obtained and are clearly seen in Figure 2. The same phases were also detected from the other composite system samples.

The measured XRD patterns of the Pb-Al-Sn system after the solidification reactions for the Pb side are seen in Figure 3. The figure shows that the XRD spectrums of the lead-rich samples are very similar to the XRD patterns of the pure lead substance. The crystal structures and symmetry type of the samples were indexed in face-central cubic (fcc). However, very small shifts of the peak positions depending on composition were detected, which resulted in cell parameter changes. The calculated unit cell parameters were a= 4.909 Å for Pb-39 wt. % Al-20 wt. % Sn, a= 4.927 Å for Pb-38 wt. % Al-20 wt. % Sn, a= 4.931 Å for Pb-37 wt. % Al-20 wt. % Sn, a= 4.932 Å for Pb-36 wt. % Al-20 wt. % Sn and a=4.945 Å for pure Pb.

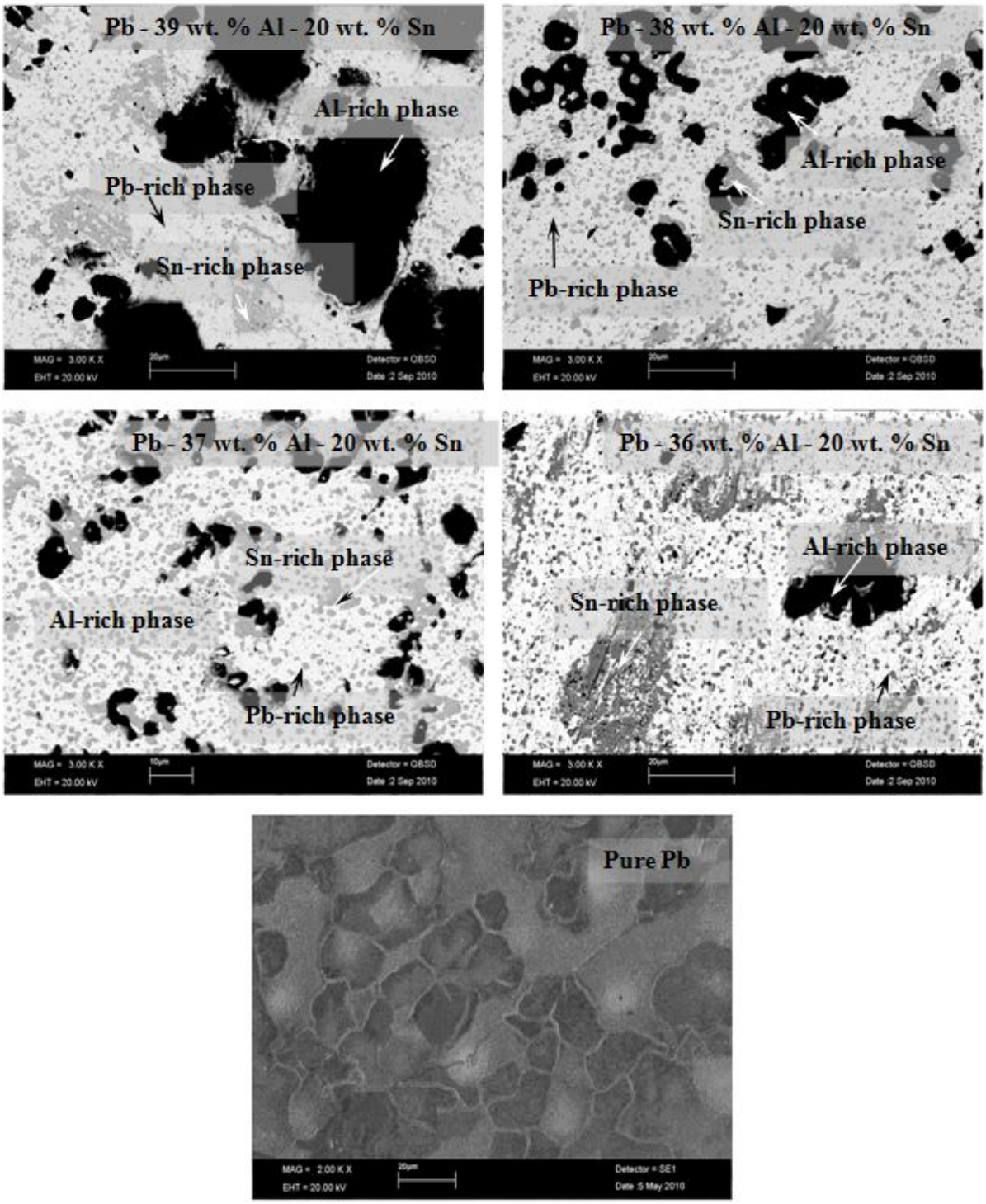

Fig.1a. The SEM images for the pure Pb and the rich Pb part of Pb-Al-Sn composite system, grey phase (Sn-rich phase), White phase (Pb-rich phase), dark phase (Al-rich phase)

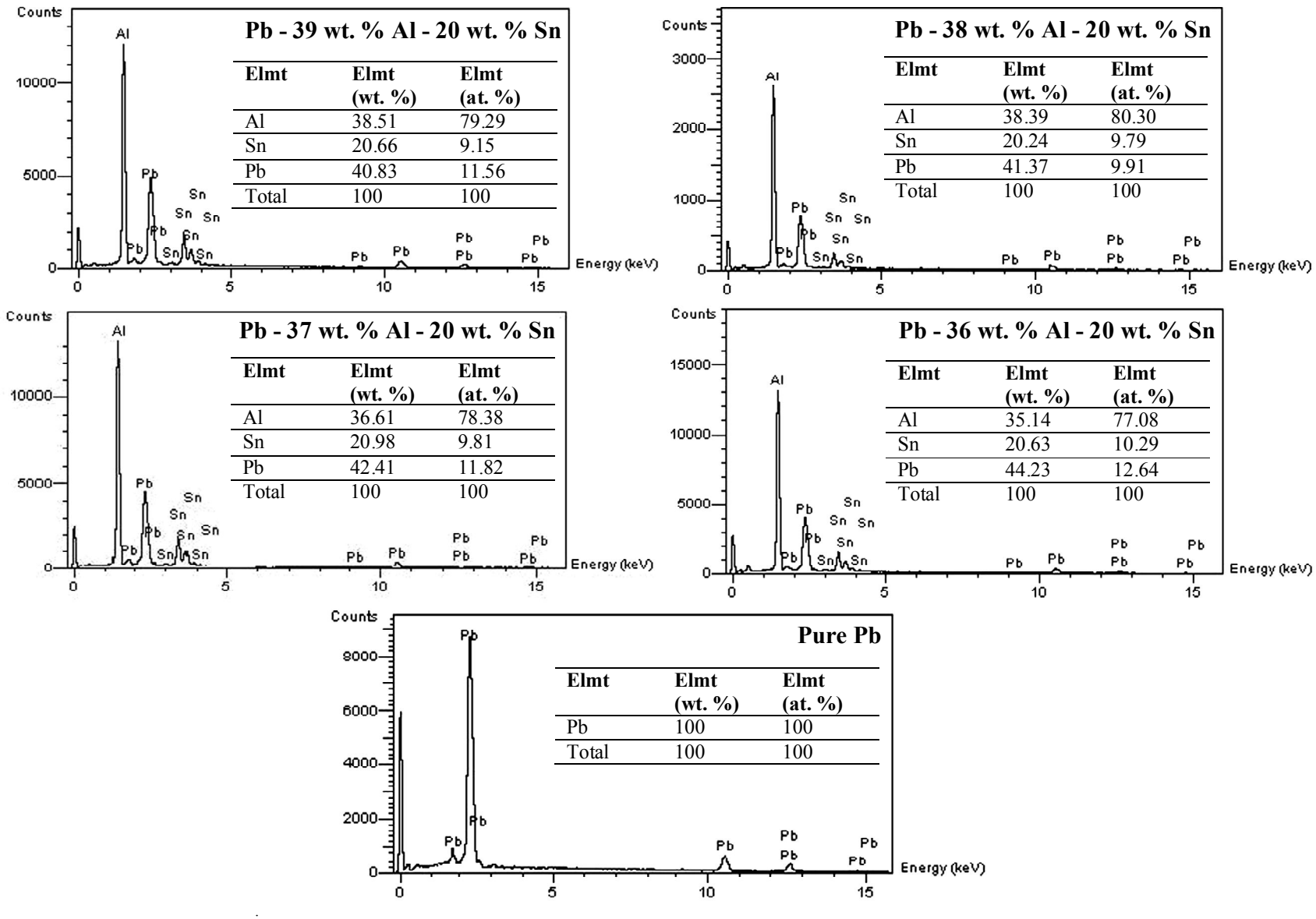

Fig.1b. The chemical compositions analysis of the pure Pb and the Pb-Al-Sn composite system for the rich Pb part by using EDX.

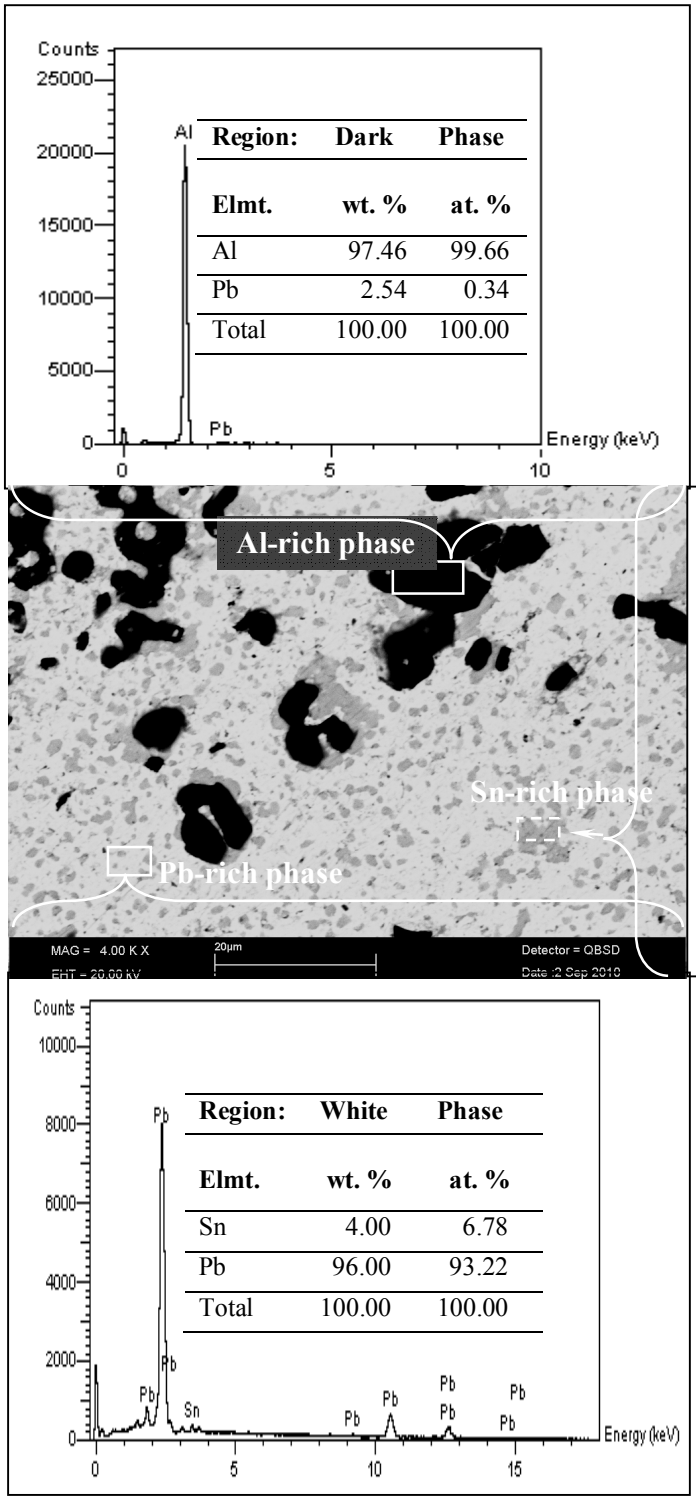

Fig.2. The chemical composition analysis of the Pb-Al-Sn composite system by using SEM, EDX, grey Phase (Sn-rich phase), dark Phase (Al-rich phase) and white phase (Pb-rich phase) for the Pb-20 wt. % Sn-38 wt. % Al.

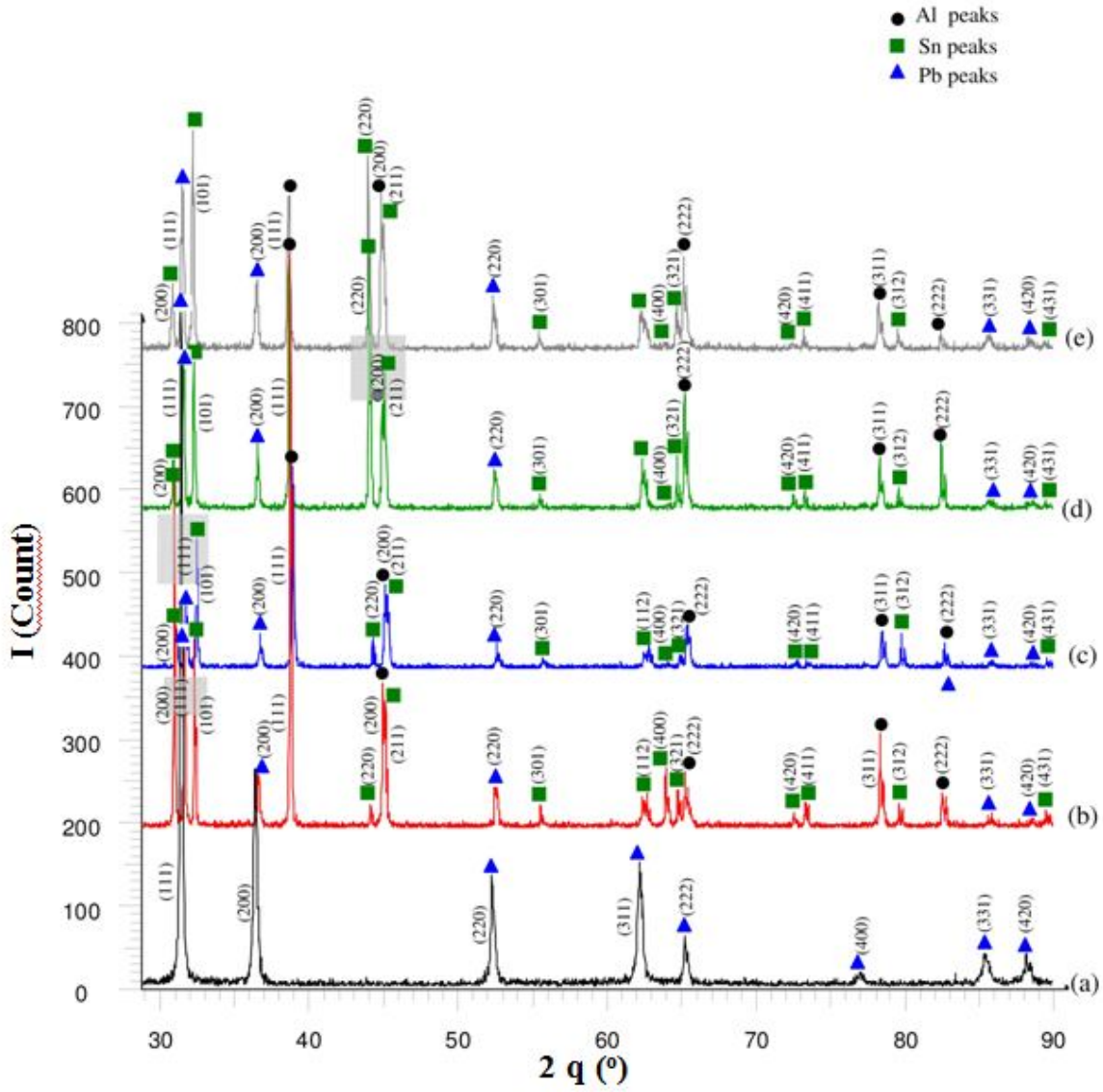

Fig.3. The measured XRD patterns for lead-weighted side of the Pb-Al-Sn composite system (a) pure Pb (b) Pb- 36 wt. % Al -20 wt. % Sn, (c) Pb- 37 wt. % Al -20 wt. % Sn, (d) Pb- 38 wt. % Al -20 wt. % Sn, (e) Pb- 39 wt. % Al -20 wt. % Sn.

The grain sizes of the samples were obtained between 66.75-92.15 nm. Also, the melting temperatures were measured between 198.55-330.48 ^{o}C. The XRD patterns of Pb-Al-Sn composite system were compared with other similar works [22-25]. The results are consistent with the results of Su et al. [22], Meydaneri et al. [23] and Swanson and Tatge [25].

The grain size of the samples was also calculated from the higher intensity peaks of the XRD pattern (111), (200), (222), (331). The values of the grain sizes were between 66.75-92.15 nm and are given in Table 1.

Additionally, the melting temperatures of the samples were precisely determined by using a DSC apparatus, which is shown in Figure 4, and are given in Table 1. The electrical conductivity versus temperature curves were plotted for the samples with constant tin concentration, obtained in the temperature range between room temperature and melting point. Figure 5 shows the electrical conductivity results for four composite system samples and the pure Pb sample. The samples for the constant tin concentrations, and electrical conductivity were obtained between 1.20×10^{6} $(\Omega m)^{-1}$-6.25×10^{6} $(\Omega m)^{-1}$. Conductivity decreases almost linearly with decreasing temperature which indicates that the samples have a metallic type of conductivity. Figure 5 also shows the results of other studies [23, 24] and indicates the consistency of all the results.

The TCR of the samples was calculated by using the electrical resistivity values which were in the range of 3.15-4.60 $\times 10^{-3} K^{-1}$. The obtained results are consistent with the results of Raymond [26]. The results of all deduced physical quantities are given in Table 1.

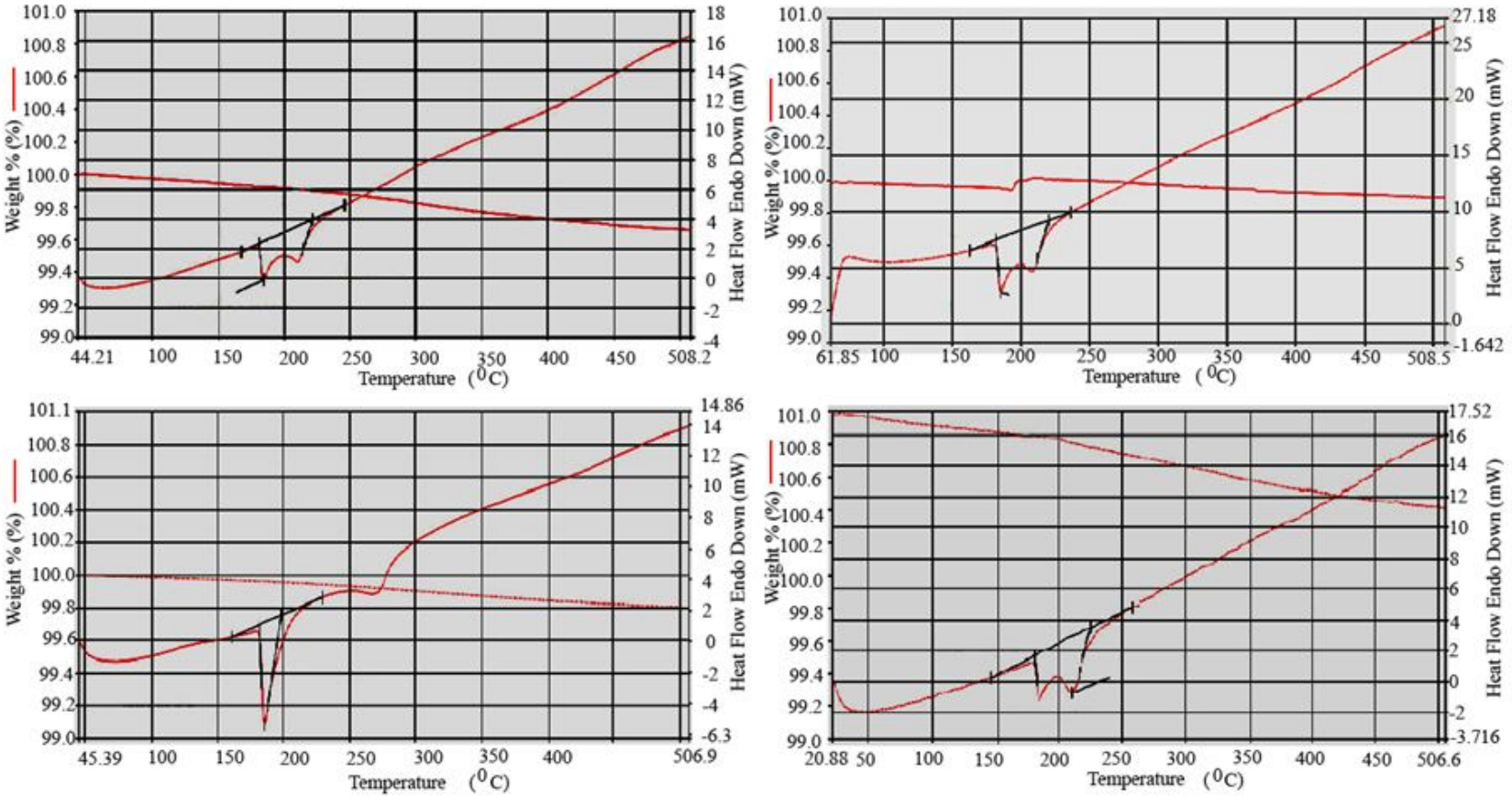

Fig.4. Heat flow curve versus the temperature for Pb-Al-Sn composite system.

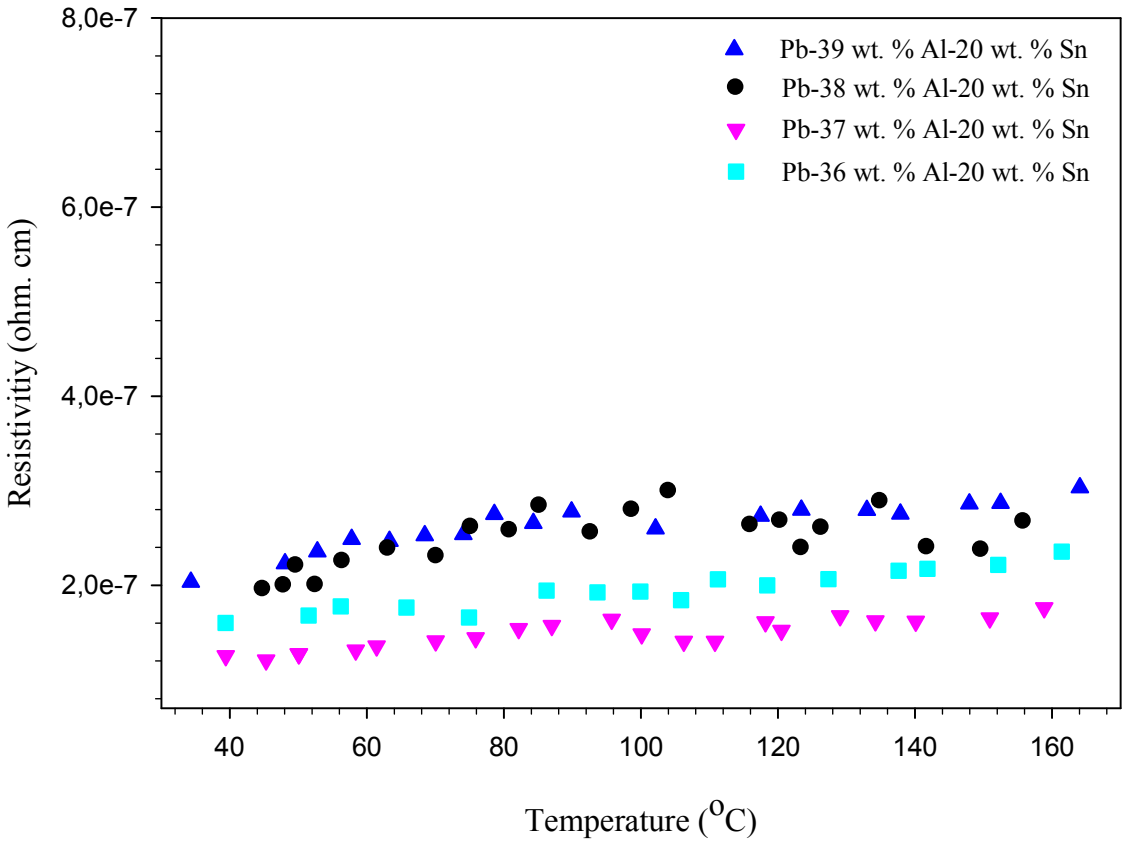

Fig. 5. Electrical resistivity of the pure Pb and the Pb-Al-Sn composite systems versus temperature for constant tin concentration.

Table 1. Electrical resistivity and temperature coefficient of resistivity at 310 K and 440 K for the Pb-Al-Sn composite systems.

Samples	Melting temperature (°C)	Unit cell parameters $a\,(\mathring{A})$	Grain Size (nm)	Electrical conductivity σ $(10^6\,\Omega^{-1}m^{-1})$		Temperature coefficient of resistivity, $\alpha\,(10^{-3}\,K^{-1})$
				T=310 K	T=440 K	Δ T=310 K -440 K
Pb-39 wt. % Al-20 wt. % Sn	222.04	4.909	92.15	3.11	2.09	3.73
Pb-38 wt. % Al-20 wt. % Sn	220.28	4.927	80.33	3.79	2.37	4.60
Pb-37 wt. % Al-20 wt. % Sn	198.55	4.931	70.50	5.05	3.59	3.15
Pb-36 wt. % Al-20 wt. % Sn	225.80	4.932	70.00	6.25	4.25	3.61
Pure Pb	330.48	4.945 4.95060[24]	66.75	2.50	1.20	-4.00

Acknowledgments. This work was financially supported by Erciyes University's Research Fund, Project FBD-10-3262, FBA-11-3408 and FBA-11-3525. The authors would like to thank Erciyes University's Technological Research and Development Center for their technical support. Also, the authors would like to thank Prof. Dr. Yıldırım Aydoğdu for their contribution to this study.

REFERENCES

[1] Y. Ogita, Y. Ido, and M. Sakamoto, "Improvement of aluminium-lead bearings", Metal Powder Rep. 46 (2) (1991) 37–44.

[2] S. Mohan, V. Agarwala, and S. Ray, "Friction characteristics of stir-cast Al-Pb alloys", Wear 157 1 (1992) 9-17.

[3] M. Zhu, Y. Gao, C.Y. Chung, Z.X. Che, K.C. Lou, and B.L. Li, "Improvement of the wear behavior of Al-Pb alloys by mechanical alloying", Wear 242 (1-2) (2000) 47-53.

[4] M.D. Achtermann, and M.E. Greenlee, "Application of wrought lead-calcium batteries in Europe" , J. Power Sources 33 (1-4) (1991) 87-92.

[5] J. Wirtz, "New developments in continuous cast grids, Proc. 7 th. Int. Lead Conf., Madrid, Spain, 1980, D. Lambert, Batteries Int. Oct.)(1992) p.36; Wirtz J. Batteries Int, (Jan) (1996) 56-63.

[6] R.D. Prengaman, "Challenges from corrosion-resistant grid alloys in lead acid battery manufacturing", J. Power Sources 95 1-2 (2001) 224-233.

[7] A.B. Ziya, and K. Ohshimab, "X-ray diffraction study of the structure and thermal parameters of the ternary Au–Ag–Pd alloys" J. Alloys and Compd. 425 1-2 (2006) 123-128.

[8] P. Grima Gallardo, K. Ca´rdenas, M. Quintero, J. Ruiz, and G.E. Delgado, "X-ray diffraction studies on $(CuAlSe_2)_X(FeSe)_{1-X}$ alloys", Mater. Res. Bull.36 (2001) 861–866.

[9] P. Scherrer, Göttinger Nachrichten Gesell. 2 (1918) 98-100.

[10] M.R. Pinasco, E. Cordano, and M. Giovannini, "X-ray diffraction and microstructural study of PFM precious metal dental alloys under different metallurgical conditions", J. Alloys Compd. 289 (1999) 289–298.

[11] E. Antolini, and F. Cardellini, "Formation of carbon supported PtRu alloys: an XRD analysis" J. Alloys Compd. 315 (2001) 118–122.

[12] J.H. Kim, Y.M. Im, J.P. Noh, S.Miyazaki, and and T.H. Nam, ""Microstructures and martensitic transformation behavior of Ti-Ni-Sn alloys" Scripta Mater. 65 (2011) 608–610.

[13] K. Masayuki, E. Matsubara, J. Saida, M. Nakayama, K. Uematsu, T. Zhang, and et al. "Crystallisation behaviour of Cu60Zr30Ti10 bulk glassy alloy" Mat. Sci.Eng. A 375–377 (2004) 744–748.

[14] V.P. Sinha, P.V. Hegde, G.J. Prasad, G.K. Dey, and H.S. Kamath, "Phase transformation of metastable cubic γ-phase in U–Mo alloys" J. Alloys Compd. 506 (2010) 253–262.

[15] M. Geetha, A.K. Singh, A.K. Gogia, and R. Asokamani, "Effect of thermomechanical processing on evolution of various phases in Ti–Nb–Zr alloys" J. Alloys Compd. 384 (2004)131–144.

[16] A. Patterson, Phys. Rev. 56 (1939) 978-982.

[17] M. Arı, B. Saatçi, M. Gündüz, F. Meydaneri, and M. Bozoklu, "Microstructure and thermo-electrical transport properties of Cd–Sn alloys" Mater. Charact. 59 (2008) 624-630.

[18] M. Arı. B. Saatçi, M. Gündüz, M. Payveren, and S. Durmuş, "Thermoelectrical characterization of Sn–Zn alloys" Mater. Charact. 59 (2008) 757-763.

[19] B. Saatçi, M. Arı, M. Gündüz, F. Meydaneri, M. Bozoklu and S. Durmuş, "Thermal and electrical conductivities of Cd Zn alloys " J. Phys.:Condens. Matter. 18 (2006)10643-10653.

[20] B. D. Cullity, Elements of X-Ray diffraction, third printing Addison-Wesley Publishing Company, Inc. United State of America, 1967.

[21] F. M. Smits, "Measurement of Sheet Resistivities with the Four-Point Probe" The Bell sys. Tech. J. (1958) 711-718.

[22] T. Su, X. Jia, H. Ma, J. Guo, Y. Jiang, N. Dong, and et al. "Thermoelectric properties of nonstoichiometric PbTe prepared by HPHT" J. Alloys and Compd. 468 (2009) 410-413.

[23] F. Meydaneri, B. Saatçi and M. Arı, "Thermo-Electrcial Characterization Of Lead-Cadmium (Pb-Cd) Alloys" Int. J.Phys. Sci. 7 48 (2012) 6210-6221.

[24]Y. Ocak, S. Aksöz, N. Maraşlı, and E. Çadırlı, "Dependency of thermal and electrical conductivity on the temperature and composition of Sn in the Pb−Sn alloys" Fluid Phase Equilibria, 295, 1, (2010) 60-67.

[25] H. E. Swanson and E. Tatge, Natl. Bur. Stand. Circ. (U.S.), 539, (1953) 34.

[26] A. S. Raymond, (1998) Principles of Physics (2 nd. Ed.) Fort Worth, Texas; London: Sounders College pub. p.602.